

Analysis and Implementation of bidirectional DC to DC Converter by using Fuzzy logic Controller

Ganji Sai Kumar¹, G. Ramudu², D. Vijay Arun³

¹ Department of EEE, Gudlavalleru Engineering College. A.P.

² Asst..Professor, Department of EEE, StAnn's College of engineering and technology., A.P.

³ Asst..Professor, Department of EEE, Gudlavalleru Engineering College. A.P.

ABSTRACT

The circuit configuration of the proposed converter is very simple. The proposed converter employs a coupled inductor with same winding turns in the primary and secondary sides. Many bidirectional dc–dc converters have been researched. The bidirectional dc–dc flyback converters are more attractive due to simple structure and easy control. However, these converters suffer from high voltage stresses on the power devices due to the leakage inductor energy of the transformer. The objective of this proposed methodology is to develop fuzzy logic controller on control boost dc-dc converter using MATLAB@Simulink software. The fuzzy logic controller has been implemented to the system by developing fuzzy logic control algorithm. The design and calculation of the components especially for the inductor has been done to ensure the converter operates in continuous conduction mode. The evaluation of the output has been carried out and compared by software simulation using MATLAB software between the open loop and closed loop circuit. The simulation results are shown that voltage output is able to be control in steady state condition for boost dc-dc converter by using this methodology

INDEX TERMS—Bidirectional dc–dc converter, coupled inductor.

Date of Submission: 02 June 2014



Date of Publication: 15 June 2014

I. INTRODUCTION

DC-DC converters are electronic devices used whenever we want to change DC electrical power efficiently from one voltage level to another. They are needed because unlike AC, DC cannot simply be stepped up or down using a transformer. In many ways, a DC-DC converter is the equivalent of a transformer.

The dc-dc converters can be viewed as dc transformer that delivers a dc voltage or current at a different level than the input source. Electronic switching performs this dc transformation as in conventional transformers and not by electromagnetic means. The dc-dc converters find wide applications in regulated switch-mode dc power supplies and in dc motor drive applications.

DC-DC converters are non-linear in nature. The design of high performance control for them is a challenge for both the control engineering engineers and power electronics engineers. In general, a good control for dc-dc converter always ensures stability in arbitrary operating condition. Moreover, good response in terms of rejection of load variations, input voltage changes and even parameter uncertainties is also required for a typical control scheme.

After pioneer study of dc-dc converters, a great deal of efforts has been directed in developing the modeling and control techniques of various dc-dc converters. Classic linear approach relies on the state averaging techniques to obtain the state-space averaged equations. From the state-space averaged model, possible perturbations are introduced into the state variables around the operating point. On the basis of the equations, transfer functions of the open-loop plant can be obtained. A linear controller is easy to be designed with these necessary transfer functions based on the transfer function.

DC to DC converters are important in portable electronic devices such as cellular phones and laptop computers, which are supplied with power from batteries primarily. Such electronic devices often contain several sub-circuits, each with its own voltage level requirement different than that supplied by the battery or an external supply (sometimes higher or lower than the supply voltage, and possibly even negative voltage). Additionally, the battery voltage declines as its stored power is drained. Switched DC to DC converters offer a method to increase voltage from a partially lowered battery voltage thereby saving space instead of using multiple batteries to accomplish the same thing.

DC-DC converters are electronic devices that are used whenever we want to change DC electrical power efficiently from one voltage level to another. In the previous chapter we mentioned the drawbacks of doing this with a linear regulator and presented the case for SMPS. Generically speaking the use of a switch or switches for the purpose of power conversion can be regarded as a SMPS. From now onwards whenever we mention DC-DC Converters we shall address them with respect to SMPS.

A few applications of interest of DC-DC converters are where 5V DC on a personal computer motherboard must be stepped down to 3V, 2V or less for one of the latest CPU chips; where 1.5V from a single cell must be stepped up to 5V or more, to operate electronic circuitry. In all of these applications, we want to change the DC energy from one voltage level to another, while wasting as little as possible in the process. In other words, we want to perform the conversion with the highest possible efficiency.

DC-DC Converters are needed because unlike AC, DC can't simply be stepped up or down using a transformer. In many ways, a DC-DC converter is the DC equivalent of a transformer. They essentially just change the input energy into a different impedance level. So whatever the output voltage level, the output power all comes from the input; there's no energy manufactured inside the converter. Quite the contrary, in fact some is inevitably used up by the converter circuitry and components, in doing their job.

Modern electronic equipment and systems are made up of high-density circuitry, which requires a low voltage and high current to function. For the proper operation of this type of loads, a power supply must be able to provide a constant voltage over a wide current range and possess excellent regulation characteristics in both steady and transient states. Modeling and simulation have played an important role in the design of modern DC-DC converter. They allow the converter performance to be evaluated before the actual circuit is built. Hence, design flaws, if any, can be detected and corrected at the early stages in the design process, leading to the increased productivity and cost saving.

Modeling and simulation of DC-DC converters can be modeled in two simulations they are

- Switched Simulation
- Average Simulation

In the Switched simulation, switching action of the converters is simulated and the results are waveforms with switching ripples resembles to those found in actual converters.

In Average simulation simulates only the average behavior of the converters and therefore the results are the smooth continuous waveforms that represent an average value of the interested quantities. It is well known that the averaged simulation yields a much faster computer run time than the switched simulation.

Hence, the averaged simulation is often used in the evaluation of overall dynamic performance of the converters. In the past, the average simulation is mostly performed in SPICE. The drawback of using SPICE is that the model to be simulated must be translated into an equivalent circuit which can become difficult if the model is described by complicated equations. Although the newer versions of SPICE program provide commands to support mathematical based models, their capability is still somewhat limited.

In this State-Space Modeling of a Buck Converter can be modeled by using three modeling techniques. They are,

- O VOLTAGE MODE CONTROL
- O CURRENT MODE CONTROL
- O AVERAGE CURRENT MODE CONTROL

DC/DC switching power converters working in both continuous (CCM) and discontinuous (DCM) conduction modes. The model is based on two PWM switch sub-models commutating between them as a consequence of the operating conditions. In the modeling technique, emphasis is made in the discontinuous conduction mode and in the determination of the instants to switch between the continuous and discontinuous conduction mode sub-models. The model is used in a multilevel simulator where behavioral descriptions are permitted. Results are obtained and compared with device level simulations. These results show good accuracy and significant reduction in the simulation time.

Step-Up mode

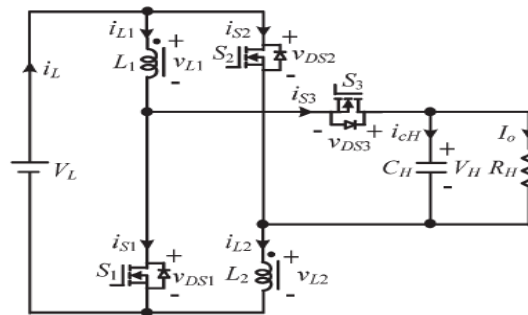


Fig.1: Proposed converter in step-up mode

The proposed converter in step-up mode is shown in Fig. 1. The pulse width modulation (PWM) technique is used to control the switches S1 and S2 simultaneously. The switch S3 is the synchronous rectifier.

Since the primary and secondary winding turns of the coupled inductor is same, the inductance of the coupled inductor in the primary and secondary sides are expressed as

$$L1 = L2 = L. \quad \text{----- (1)}$$

Thus, the mutual inductance M of the coupled inductor is given by

$$M = k\sqrt{L1L2} = kL \quad \text{-- (2)}$$

where k is the coupling coefficient of the coupled inductor. The voltages across the primary and secondary windings of the coupled inductor are as follows:

$$\begin{aligned} v_{L1} &= L1 \frac{di_{L1}}{dt} + M \frac{di_{L2}}{dt} = L \frac{di_{L1}}{dt} + kL \frac{di_{L2}}{dt} \\ v_{L2} &= M \frac{di_{L1}}{dt} + L2 \frac{di_{L2}}{dt} = kL \frac{di_{L1}}{dt} + L \frac{di_{L2}}{dt}. \end{aligned} \quad \text{----- (3)}$$

Fig.2 shows some typical waveforms in continuous conduction mode (CCM) and discontinuous conduction mode (DCM). The operating principles and steady-state analysis of CCM and DCM are described as follows.

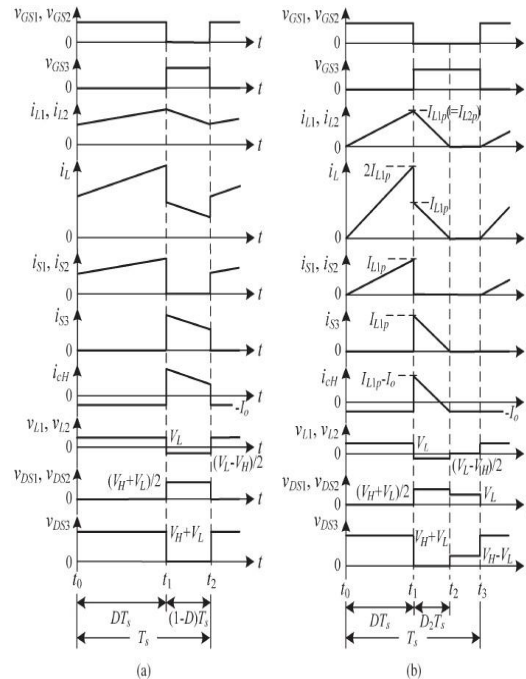


Fig.2: Some typical waveforms of the proposed converter in step-up mode. (a) CCM operation. (b) DCM operation

CCM Operation

a) Mode 1: During this time interval [t0, t1], S1 and S2 are turned on and S3 is turned off. The current flow path is shown in Fig.3(a). The energy of the low-voltage side VL is transferred to the coupled inductor. Meanwhile, the primary and secondary windings of the coupled inductor are in parallel. The energy stored in the capacitor CH is discharged to the load. Thus, the voltages across L1

$$\frac{di_{L1}(t)}{dt} = \frac{di_{L2}(t)}{dt} = \frac{V_L}{(1+k)L}, \quad t_0 \leq t \leq t_1.$$

and L2 are obtained as $v_{L1} = v_{L2} = V_L$.

----- (4)

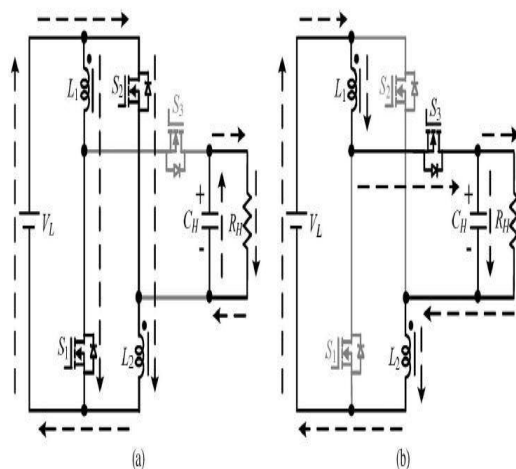


Fig 3: Current flow path of the proposed converter in step-up mode. (a) Mode 1 (b) Mode 2

b) Mode 2: During this time interval [t1, t2], S1 and S2 are turned off and S3 is turned on. The current flow path is shown in Fig.3(b). The low- voltage side VL and the coupled inductor are in series to transfer their energies to the capacitor CH and the load. Meanwhile, the primary and secondary windings of the coupled inductor are in series. Thus, the following equations are found to be

$$i_{L1} = i_{L2}$$

$$v_{L1} + v_{L2} = V_L - V_H. \quad \text{----- (5)}$$

$$\frac{di_{L1}(t)}{dt} = \frac{di_{L2}(t)}{dt} = \frac{V_L - V_H}{2(1+k)L}, \quad t_1 \leq t \leq t_2. \quad \text{----- (6)}$$

By using the state-space averaging method, the following equation is derived:

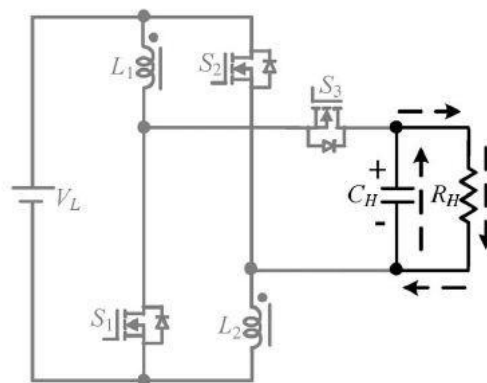


Fig.4(c) : Mode 3 for DCM operation

DCM Operation

a) Mode 1: During this time interval [t0, t1], S1 and S2 are turned on and S3 is turned off. The current flow path is shown in Fig.3 (a). The operating principle is same as that for the mode b) 1 of CCM operation. From (6), the two peak currents through the primary and secondary windings of the coupled inductor are given by

$$I_{L1p} = I_{L2p} = \frac{V_L D T_s}{(1+k)L}. \quad \text{----- (7)}$$

c) Mode 2: During this time interval [t1, t2], S1 and S2 are turned off and S3 is turned on. The current flow path is shown in Fig. 3(b). The low- voltage side VL and the coupled inductor are in series to transfer their energies to the capacitor CH and the load. Meanwhile, the primary and secondary windings of the coupled inductor are in series. The currents iL1 and iL2 through the primary and secondary windings of the coupled inductor are decreased to zero at t = t2. another expression of IL1p and IL2p is given by

$$I_{L1p} = I_{L2p} = \frac{(V_H - V_L) D_2 T_s}{2(1+k)L}. \quad \text{----- (8)}$$

Mode 3: During this time interval l [t2, t3], S1 and S2 are still turned. The current flow path is shown in Fig.3(c). The energy stored in the coupled inductor is zero. Thus, iL1 and iL2 are equal to zero. The energy stored in the capacitor CH is discharged to the load. From (12) and (13), D2 is derived as follows:

$$D_2 = \frac{2DV_L}{V_H - V_L} \quad \text{----- (9)}$$

From Fig.3(b), the average value of the output capacitor current during each switching period is given by

$$I_{cH} = \frac{\frac{1}{2}D_2T_s I_{L1p} - I_o T_s}{T_s} = \frac{1}{2}D_2 I_{L1p} - I_o \quad \text{--- (10)}$$

$$I_{cH} = \frac{D^2 V_L^2 T_s}{(1+k)L(V_H - V_L)} - \frac{V_H}{R_H} \quad \text{---- (11)}$$

Since I_{cH} is equal to zero under steady state, (11) can be rewritten as follows:

$$\frac{D^2 V_L^2 T_s}{(1+k)L(V_H - V_L)} = \frac{V_H}{R_H} \quad \text{----- (12)}$$

$$\tau_{LH} \equiv \frac{L}{R_H T_s} = \frac{L f_s}{R_H} \quad \text{----- (13)}$$

Then, the normalized inductor time constant is defined as ,

where f_s is the switching frequency. the voltage gain is given by

$$G_{DCM(step-up)} = \frac{V_H}{V_L} = \frac{1}{2} + \sqrt{\frac{1}{4} + \frac{D^2}{(1+k)\tau_{LH}}} \quad \text{----- (14)}$$

Step-down mode

Fig.5 shows the proposed converter in step-down mode. The PWM technique is used to control the switch S3. The switches S1 and S2 are the synchronous rectifiers. Fig. 6 shows some typical waveforms in CCM and DCM.

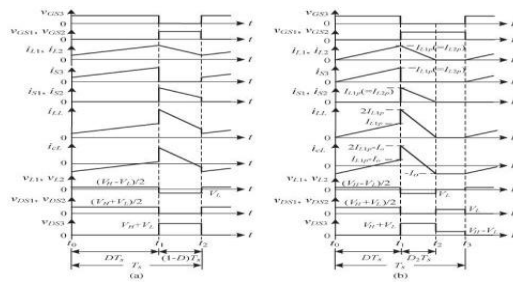


Fig.6 : Some typical waveforms of the proposed converter in step-down mode. (a) CCM operation (b) DCM operation

The operating principle and steady-state analysis of CCM and DCM are described as follows.

CCM Operation

a) Mode 1: During this time interval $[t_0, t_1]$, S3 is turned on and S1/S2 are turned off. The current flow path is shown in Fig.7(a).

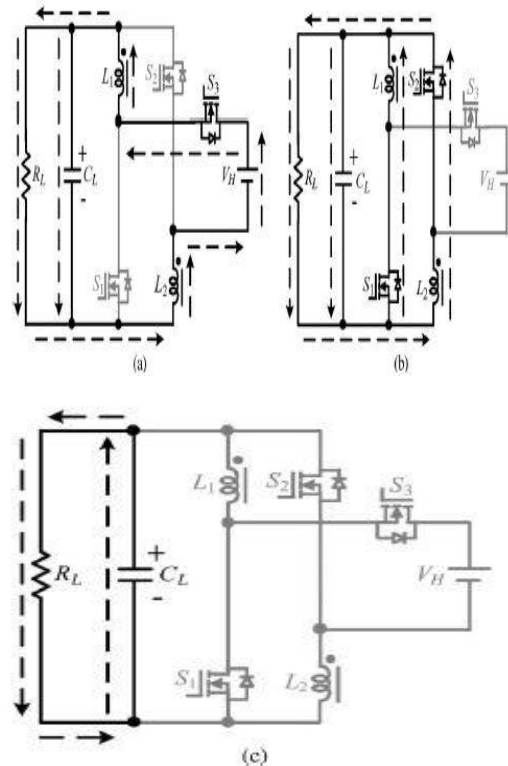


Fig.7: Current flow path of the proposed converter in step-down mode. (a) Mode 1. (b) Mode 2. (c) Mode 3 for DCM operation

a) Mode1: The energy of the high-voltage side V_H is transferred to the coupled inductor, the capacitor C_L , and the load. Meanwhile, the primary and secondary windings of the coupled inductor are in series.

b) Mode 2: During this time interval $[t_1, t_2]$, S_3 is turned off and S_1/S_2 are turned on. The current flow path is shown in Fig.7(b). The energy stored in the coupled inductor is released to the capacitor C_L and the load. Meanwhile, the primary and secondary windings of the coupled inductor are in parallel.

Thus, the voltages across L_1 and L_2 are derived as

$$v_{L1} = v_{L2} = -V_L$$

DCM Operation

The operating modes can be divided into three modes, defined as modes 1, 2, and 3.

1) Mode 1: During this time interval $[t_0, t_1]$, S_3 is turned on and S_1/S_2 are turned off. The current flow path is shown in Fig.7(a). The operating principle is same as that for the mode 1 of CCM operation. the two peak currents through the primary and secondary windings of the coupled inductor are given by

$$I_{L1p} = I_{L2p} = \frac{(V_H - V_L)DT_s}{2(1+k)L}$$

----- (15)

b) Mode 2: During this time interval $[t_1, t_2]$, S_3 is turned off and S_1/S_2 are turned on. The current flow path is shown in Fig. 7(b). The energy stored in the coupled inductor is released to the capacitor C_L and the load. Meanwhile, the primary and secondary windings of the coupled inductor are in parallel. The currents i_{L1} and i_{L2} through the primary and secondary windings of the coupled inductor are decreased to zero at $t = t_2$.

another expression of I_{L1p} and I_{L2p} is given as

$$I_{L1p} = I_{L2p} = \frac{V_L D_2 T_s}{(1+k)L} \quad \text{----- (16)}$$

c) **Mode 3:** During this time interval $[t_2, t_3]$, S_3 is still turned off and S_1/S_2 are still turned on. The current flow path is shown in Fig.7(c). The energy stored in the coupled inductor is zero. Thus, i_{L1} and i_{L2} are equal to zero. The energy stored in the capacitor C_L is discharged to the load. D_2 is derived as follows:

$$D_2 = \frac{D(V_H - V_L)}{2V_L} \quad \text{----- (17)}$$

Boundary Operating Condition of CCM and DCM

When the proposed converter in step-down mode is operated in BCM, the voltage gain of CCM operation is equal to the voltage gain of DCM operation. the boundary normalized inductor time constant $\tau_{LL,B}$ can be derived as follows:

$$\tau_{LL,B} = \frac{(1-D)(2-D)}{2(1+k)} \quad \text{---- (18)}$$

The curve of $\tau_{LL,B}$ is plotted in Fig.8. If τ_{LL} is larger than $\tau_{LL,B}$, the proposed converter in the step-down mode is operated in CCM

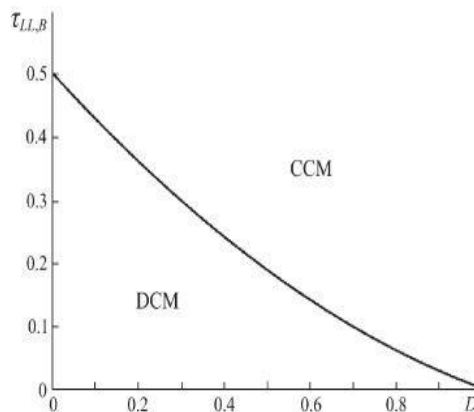


Fig.8: Boundary.condition.of.the.proposed.conv ert er.in.step-down.k=1)

Fuzzy Logic Controller for Boost Dc-Dc Converter

An analysis of boost converter circuit revealed that the inductor current plays significant task in dynamic response of boost converter. Additionally, it can provide the storage energy information in the converter. Thus, any changes on the inductor current may affect output voltage and output voltage will provide steady state condition information of converter. However, the three main parameters need to be considered when designing boost converters are power switch, inductor and capacitor. In this objective to achieve the desired output voltage and the stability is by designing the power switch.

FUZZY LOGIC MEMBERSHIP FUNCTION

The boost dc-dc converter is a nonlinear function of the duty cycle because of the small signal model and its control method was applied to the control of boost converters. Fuzzy controllers do not require an exact mathematical model. Instead, they are designed based on general knowledge of the plant. Fuzzy controllers are designed to adapt to varying operating points. Fuzzy Logic Controller is designed to control the output of boost dc-dc converter using Mamdani style fuzzy inference system. Two input variables, error (e) and change of error (de) are used in this fuzzy logic system. The single output variable (u) is duty cycle of PWM output.

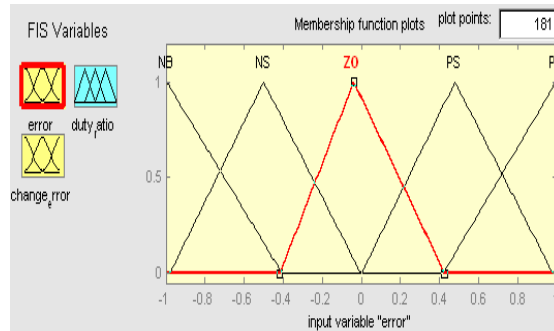


Figure 9 : The Membership Function plots of error.

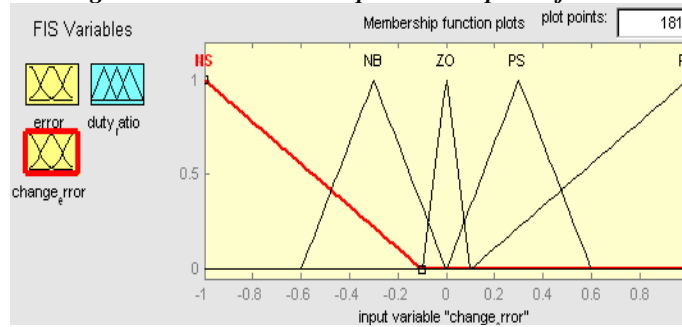


Figure 10: The Membership Function plots of change error.

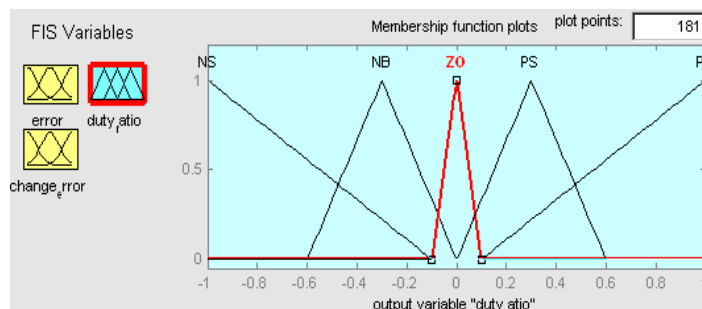


Figure 11: The Membership Function plots of duty ratio.

Fuzzy Logic Table Rules

The objective of this dissertation is to control the output voltage of the boost converter. The error and change of error of the output voltage will be the inputs of fuzzy logic controller. These 2 inputs are divided into five groups; NB: Negative Big, NS: Negative Small, ZO: Zero Area, PS: Positive small and PB: Positive Big and its parameter. These fuzzy control rules for error and change of error can be referred in the table that is shown in Table I as per below:

Table I Table rules for error and change of error.

(e) \ (de)	NB	NS	ZO	PS	PB
NB	NB	NB	NB	NS	ZO
NS	NB	NB	NS	ZO	PS
ZO	NB	NS	ZO	PS	PB
PS	NS	ZO	PS	PB	PB
PB	ZO	PS	PB	PB	PB

SIMULINK MODELS AND RESULTS SIMULATION MODEL OF CONVENTIONAL BOOST CONVERTER

The Conventional converter in step-up mode is shown in Fig 12 The pulse width modulation (PWM) technique is used to control the switches. A simulation model of a high step up DC-DC converter is shown below:

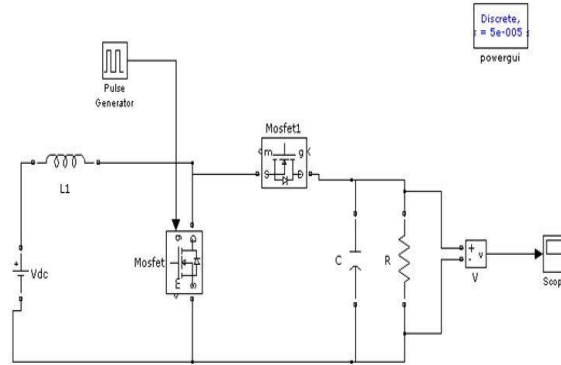


Fig.12: Simulation model of conventional boost converter Simulation Result of Conventional Boost Converter

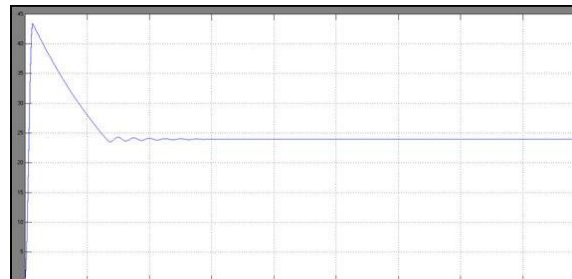
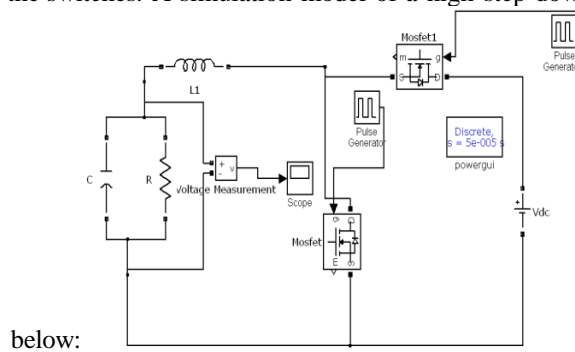


Fig.13: Output voltage of conventional Boost converter Simulation Model of Conventional Buck Converter

The Conventional converter in step-down mode is shown in Fig.14 The pulse width modulation (PWM) technique is used to control the switches. A simulation model of a high step down DC-DC converter is shown



below:

Fig.14: Simulation model of conventional buck converter Simulation Result of Conventional Buck Converter

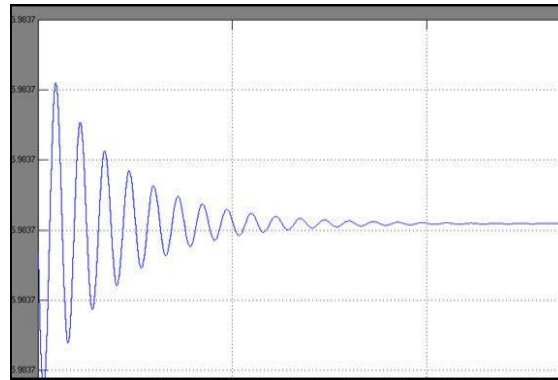


Fig.15: Output voltage of conventional Buck converter Simulation Model of Proposed Boost Converter

The proposed converter in step-up mode is shown in Fig 16 The pulse width modulation (PWM) technique is used to control the switches S1 and S2 simultaneously. The switch S3 is the synchronous rectifier. A simulation modeling of a high step up DC-DC converter is shown below

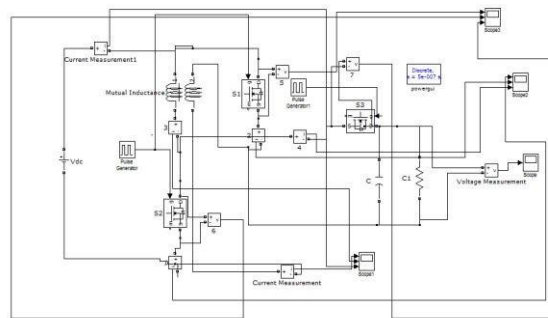


Fig.16: Simulation model of high step up DC DC converter with R load

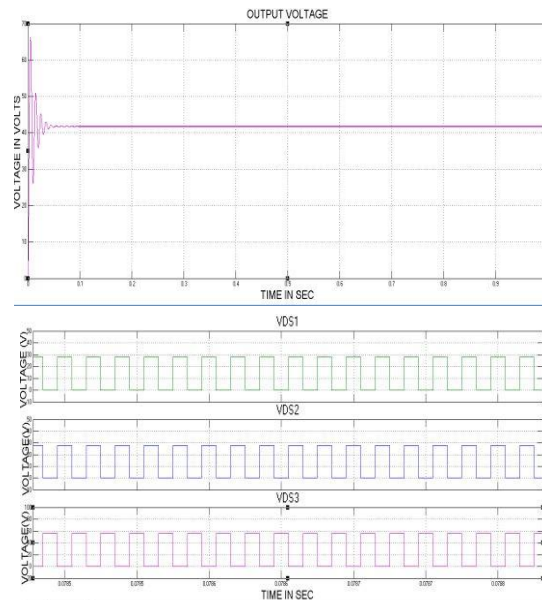


Fig.16 (a) : Output voltage of proposed Boost converter

Fig.16(a) shows the waveforms of the input current i_L and the coupled inductor currents i_{L1} and i_{L2} in step-up mode. It can be seen that i_{L1} is equal to i_{L2} . The current i_L is double of the level of the coupled-inductor current during S1/S2 ON- period and equals the coupled-inductor current during S1/S2 OFF-period.

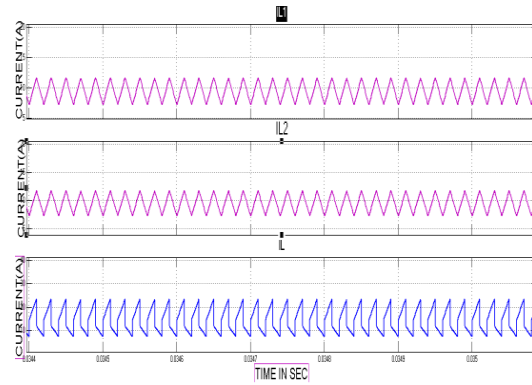


Fig.16(b) : Some experimental waveforms of the proposed converter in step-up Mode (iL1, iL2, and iL)

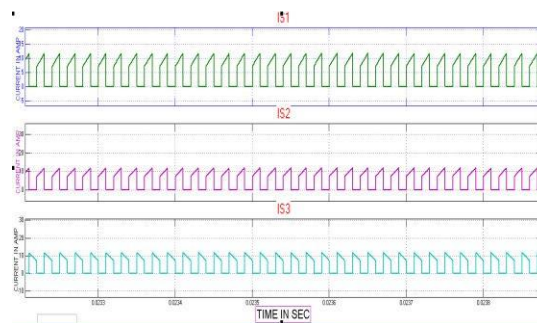


Fig.16(c): Some experimental waveforms of the proposed converter in step-up Mode (iS1, iS2, and iS3)

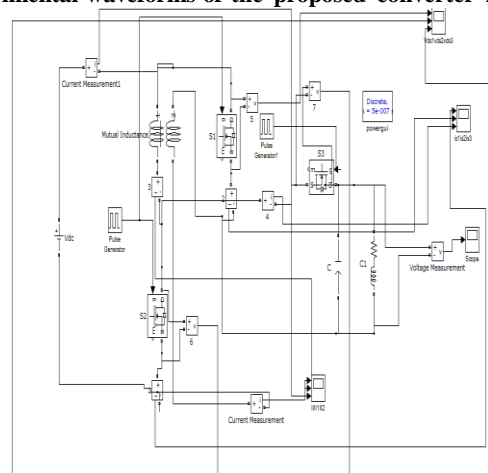


Fig.17 : Simulation model of high step up DC DC converter with RL load

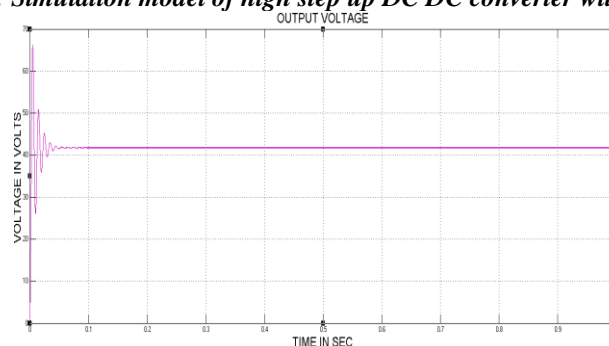


Fig.18: Output voltage of proposed Boost converter

Simulation Model of Proposed Buck Converter

Fig.5.7 shows the proposed converter in step-down mode. The PWM technique is used to control the switch S3. The switches S1 and S2 are the synchronous rectifiers. Fig. 8 shows some typical waveforms in CCM and DCM.

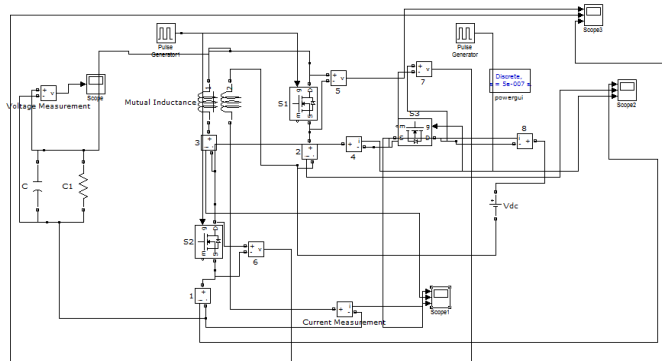


Fig.19 : Simulation model of high step down DC DC converter

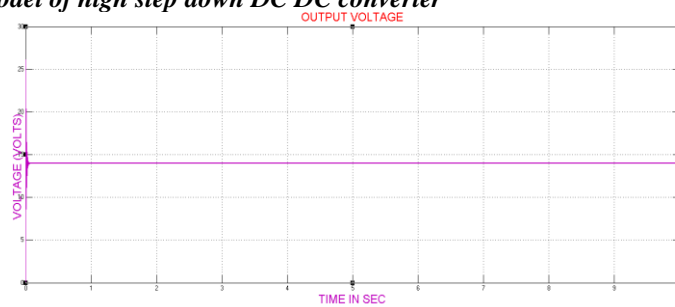


Fig.20 : Output voltage of proposed Buck converter

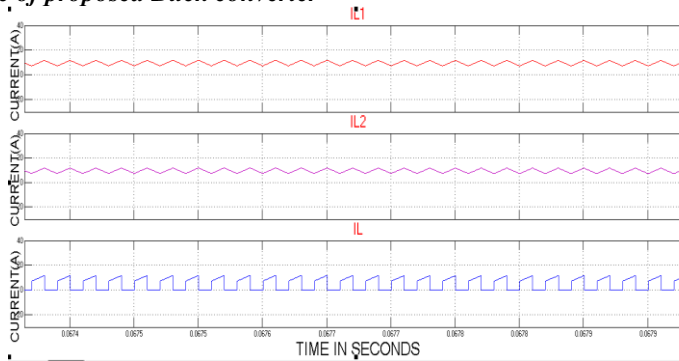


Fig.21 : Some experimental waveforms of the proposed converter in step down Mode(i_{LL} , i_{L1} , and i_{L2})

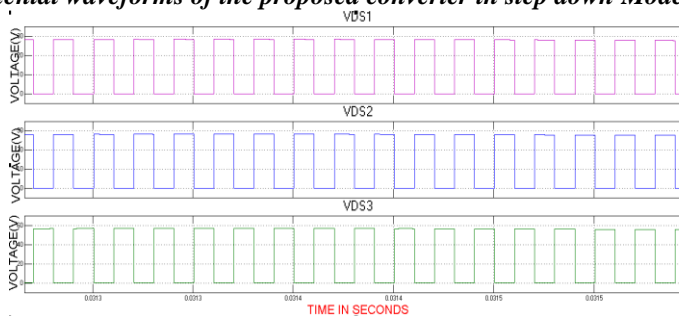


Fig.22: Some experimental waveforms of the proposed converter in step down Mode (v_{DS3} , v_{DS1} and v_{DS2})

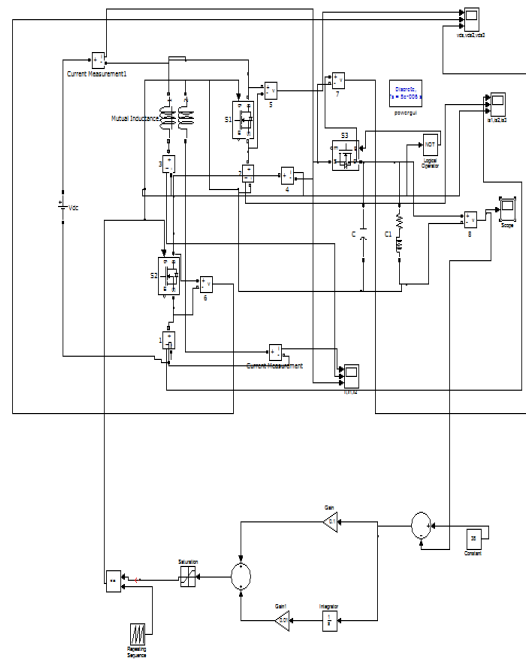


Fig.22: Simulation model of high step up DC DC converter with RL load By usng PI controller

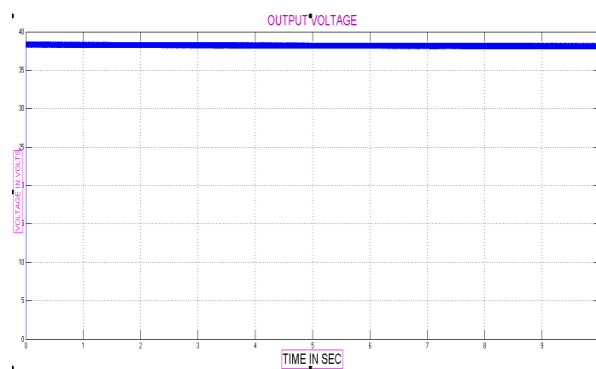


Fig.23:Output voltage of proposed Boost converter by using PI controller

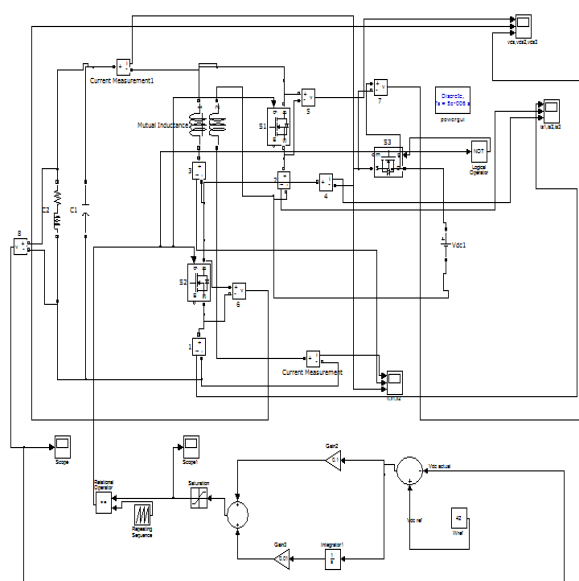


Fig.24 : Simulation model of high step down DC DC converter with RL load By usng PI controller

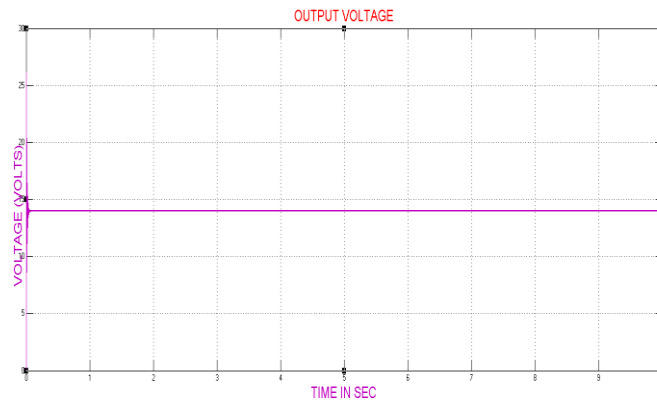


Fig.25 : Output voltage of proposed Buck converter by using PI controller

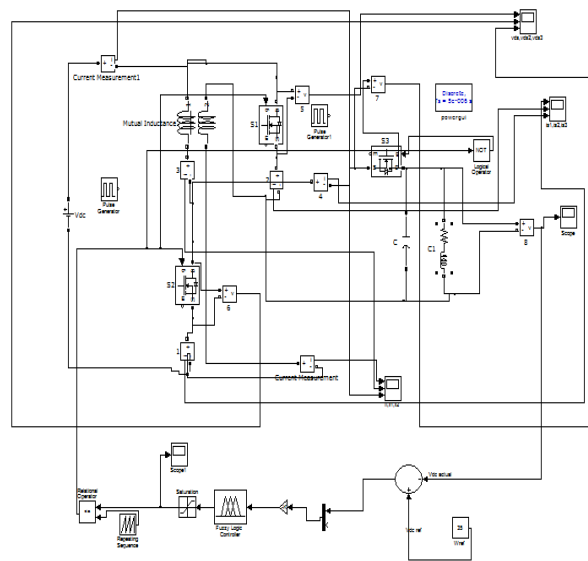


Fig.26 : Simulation model of high step up DC DC converter with RL load By using Fuzzy logic controller

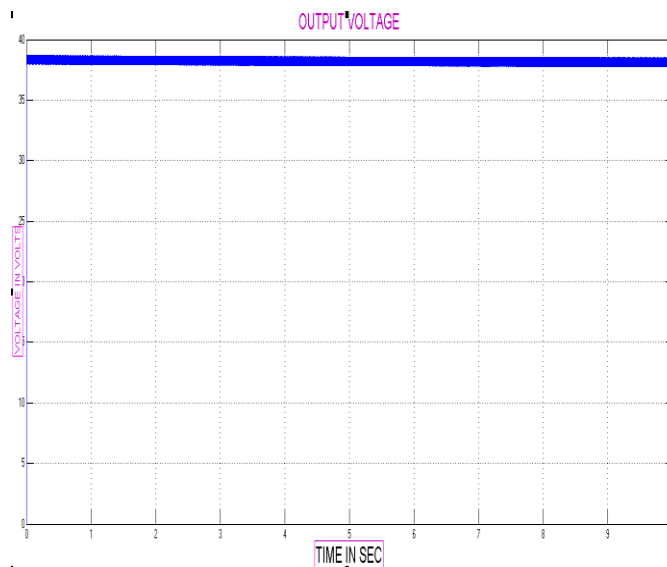


Fig.27 : Output voltage of proposed Boost converter by using Fuzzy logic controller

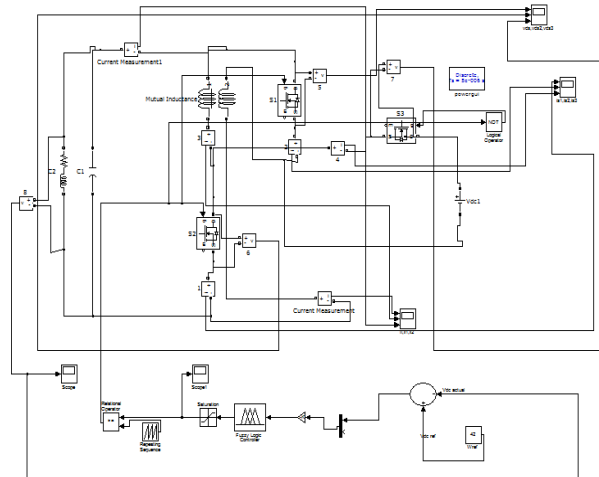


Fig.28 : Simulation model of high step down DC DC converter with RL load By using Fuzzy logic controller

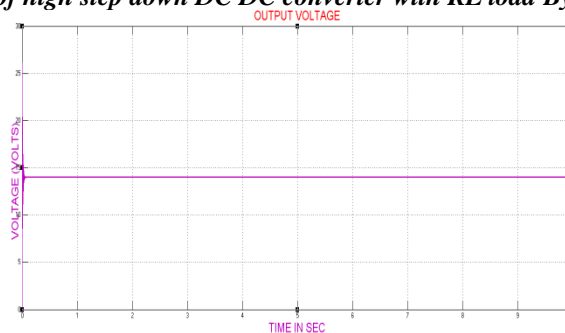


Fig.29: Output voltage of proposed Buck converter by using Fuzzy logic controller

Comparison Of The Proposed Converter And Conventional Bidirectional Buck – Boost Converter

A. VOLTAGE GAIN

The below tabular forms shows the voltage gain of the proposed converter and conventional bidirectional dc-dc boost converter.

Table.1 : Comparison of voltage gains of conventional and proposed boost converter

Duty cycle	Voltage gain (Conventional converter)	Voltage gain (Proposed converter with open loop controller)
0.2	1.25	1.5
0.4	1.66	2.33
0.5	2	3.0
0.6	2.5	4.0
0.8	5.0	9.0

The below tabular forms shows the settling times of the proposed converter with pi and fuzzy logic controller bidirectional dc-dc boost converter.

Table 5.4 Comparison of settling times of the proposed converter with pi and fuzzy logic controller bidirectional dc-dc boost converter

Input Voltage (Volts)	Output Voltage (Volts)	Settling Time Ts(Ms) (Pi Controller)	Settling Time Ts(Ms) (Fuzzy Logic Controller)
14	40	4.62	4.12
14	35	3.86	3.6
14	30	3.2	2.8

CONCLUSION

In this project a novel bidirectional dc–dc converter by using fuzzy logic controller is proposed. The circuit configuration of the proposed converter is very simple. The proposed converter has higher step-up and step-down voltage gains, lower voltage stress on the switches and lower average value of the switch current than the conventional bidirectional boost/buck converter. Design of a fuzzy logic controller on control boost dc-dc converter by using MATLAB has been successfully achieved. A simple algorithm based on the prediction of fuzzy logic controller, possibly using the fuzzy rules parameter, is showing to be more convenient than the circuit without fuzzy. Using a closed loop circuit with fuzzy logic controller, it is confirmed that the boost dc-dc converter gives a value of output voltage exactly as circuit requirement. Hence, the closed loop circuit of boost dc-dc converter controlled that by fuzzy logic controller confirmed the methodology and requirement of the proposed approach. These studies could solve many types of problems regardless on stability because as we know that fuzzy logic controller is an intelligent controller to their appliances

REFERENCES

- [1] Yan-Fei Liu, P. C. Sen. “*Digital control of switching power converters*”. Proceedings of the 2005, IEEE Conference on Control Applications, Toronto, Canada, august 28-31, 2005.
- [2] W. C., & Tse, C. K. (1996). “*Development of a fuzzy logic controller for DC/DC converters: Design, computer simulation, and experimental evaluation*”. IEEE Transactions on Power Electronics.
- [3] W. C., Tse, C. K., & Lee, Y. S. (1994). “*A fuzzy logic controller for DC–DC converter*”. In IEEE power electronics specialists conference records.
- [4] V. S. C. Raviraj, P. C. Sen, “*Comparative Study of Proportional- Integral, Sliding mode, and Fuzzy Logic Controllers for Power Converters*”. IEEE Trans on Industry Applications, Vol. 33, No. 2, March/April 1997.
- [5] K. Viswanathan, D. Srinivasan and R. Oruganti, “*A Universal Fuzzy Controller for a Non-linear Power Electronic Converter*”. IEEE International Conference on Fuzzy Systems, 2002, Vol. 1.
- [6] L. Schuch, C. Rech, H. L. Hey, H. A. rundling, H. Pinheiro, and J. R. Pinheiro, “Analysis and design of a new high-efficiency bidirectional integrated ZVT PWM converter for DC-bus and battery-bank interface,” *IEEE Trans. Ind. Appl.*, vol. 42, no. 5, pp. 1321–1332, Sep./Oct. 2006.
- [7] X. Zhu, X. Li, G. Shen, and D. Xu, “Design of the dynamic power compensation for PEMFC distributed power system,” *IEEE Trans. Ind. Electron.*, vol. 57, no. 6, pp. 1935–1944, Jun. 2010.
- [8] G. Ma, W. Qu, G. Yu, Y. Liu, N. Liang, and W. Li, “A zero-voltageswitching bidirectional dc–dc converter with state analysis and softswitching- oriented design consideration,” *IEEE Trans. Ind. Electron.*, vol. 56, no. 6, pp. 2174–2184, Jun. 2009.
- [9] F. Z. Peng, H. Li, G. J. Su, and J. S. Lawler, “A new ZVS bidirectional dc–dc converter for fuel cell and battery application,” *IEEE Trans. Power Electron.*, vol. 19, no. 1, pp. 54–65, Jan. 2004.
- [10] K. Jin, M. Yang, X. Ruan, and M. Xu, “Three- level bidirectional converter for fuel-cell/battery hybrid power system,” *IEEE Trans. Ind. Electron.*, vol. 57, no. 6, pp. 1976–1986, Jun. 2010.
- [11] R. Gules, J. D. P. Pacheco, H. L. Hey, and J. Imhoff, “A maximum power point tracking system with parallel connection for PV stand-alone applications,” *IEEE Trans. Ind. Electron.*, vol. 55, no. 7, pp. 2674–2683, Jul. 2008.
- [12] Z. Liao and X. Ruan, “A novel power management control strategy for stand-alone photovoltaic power system,” in *Proc. IEEE IPEMC*, 2009, pp. 445–449.
- [13] S. Inoue and H. Akagi, “A bidirectional dc–dc converter for an energy storage system with galvanic isolation,” *IEEE Trans. Power Electron.*, vol. 22, no. 6, pp. 2299–2306, Nov. 2007.
- [14] L. R. Chen, N. Y. Chu, C. S. Wang, and R. H. Liang, “Design of a reflexbased bidirectional converter with the energy recovery function,” *IEEE Trans. Ind. Electron.*, vol. 55, no. 8, pp. 3022–3029, Aug. 2008.
- [15] S. Y. Lee, G. Pfaelzer, and J. D. Wyk, “Comparison of different designs of a 42-V/14-V dc/dc converter regarding losses and thermal aspects,” *IEEE Trans. Ind. Appl.*, vol. 43, no. 2, pp. 520–530, Mar./Apr. 2007.
- [16] K. Venkatesan, “Current mode controlled bidirectional flyback converter,” in *Proc. IEEE Power Electron. Spec. Conf.*, 1989, pp. 835–842.
- [17] T. Qian and B. Lehman, “Coupled input-series and output-parallel dual interleaved flyback converter for high input voltage application,” *IEEE Trans. Power Electron.*, vol. 23, no. 1, pp. 88–95, Jan. 2008.
- [18] G. Chen, Y. S. Lee, S. Y. R. Hui, D. Xu, and Y. Wang, “Actively clamped bidirectional flyback converter,” *IEEE Trans. Ind. Electron.*, vol. 47, no. 4, pp. 770–779, Aug. 2000.
- [19] F. Zhang and Y. Yan, “Novel forward-flyback hybrid bidirectional dc–dc converter,” *IEEE Trans. Ind. Electron.*, vol. 56, no. 5, pp. 1578–1584, May 2009.

Author profiles



Ganji Sai Kumar received the B.Tech in EEE from VR Siddartha Engineering College. Pursuing M.Tech in Power electronics and electrical drives from Gudlavalleru Engineering College.



D.Vijay Arun received the B.Tech in EEE SVH Engineering College. M.Tech in Electrical Power Systems from Narasaraopet Engineering College. Present he is working as an Asst. Prof in Gudlavalleru Engineering college, a.p, India.



G.Ramudu has received the B.tech in EEE VRS & YRN College of Engineering and Technology. M.Tech in Power Electronics and Electric Drives from Vignan's Engineering college. Present he is working as an Asst. Prof in St. Ann's college of Engineering and technology, a.p, India.